International Journal of Thermophysics, Vol. 19, No. 4, 1998

Interfaces Between Two or Three Coexisting Fluid Phases in the System Methane–Perfluoromethane: Calculations with the Born–Green–Yvon Equation[1]

M. Wendland[2]

Wetting is studied for the binary mixture methane–perfluoromethane (CH_4–CF_4) with the Born–Green–Yvon (BGY) equation in the attractive mean field approximation (AMFA). The general phase behavior is consistent with the AMFA equation of state. Close to a three-phase equilibrium L_1L_2V, perfect wetting of the interface L_1V by the second liquid phase L_2 occurs. Liquid–vapor and liquid–liquid interfaces in the vincinity of the three-phase equilibrium are calculated with the BGY equation, and the surface tension is estimated from the density profiles. The results are compared to previous investigations of wetting in fluid systems, especially the theory of Cahn.

KEY WORDS: binary mixture; Born–Green–Yvon equation; liquid–vapor interfaces; methane; perfluoromethane; statistical mechanics; surface tension; wetting.

1. INTRODUCTION

It was shown in a previous paper [1] that the Born–Green–Yvon (BGY) equation in the attractive mean field approximation (AMFA) by Fischer and Methfessel [2] is consistent with a van der Waals-type equation of state, the AMFA equation of state, for both pure fluids and binary mixtures. Moreover, BGY results agree quite well with bulk phase equilibrium simulations with the NPT + test particle method for pure fluids and model mixtures and with liquid–vapor interface simulations for pure fluids

---

[1] Paper presented at the Thirteenth Symposium on Thermophysical Properties, June 22–27, 1997, Boulder, Colorado, U.S.A.

[2] Institut für Land-, Umwelt- und Energietechnik, Universität für Bodenkultur, Nussdorfer Lände 29-31, A-1190 Wien, Austria.

0195-928X/98/0700-1197$15.00/0

and argon–krypton mixtures. In a second paper [3] the binary mixture methane–perfluoromethane (CH_4–CF_4) was studied with the BGY equation and the AMFA equation of state. In addition to liquid–vapor interfaces, interfaces between two liquids or two liquids and a vapor phase were found. For liquid–vapor interfaces close to the liquid–liquid–vapor equilibrium, wetting was observed. While increasing the bulk liquid concentration of CH_4 towards the value of the three-phase equilibrium, a layer shows up in the interface and increases in thickness. Close to the three-phase equilibrium this layer has a thickness of about 55 molecular diameters.

Wetting and wetting transitions have been studied thoroughly theoretically and experimentally. Wetting has been found at solid–gas interfaces by gradient theory (e.g., Teletzke et al. [4]), BGY equation (e.g., Wendland et al. [5]), density functional (DF) theory (e.g., Dhawan et al. [6]), and molecular simulation (e.g., Sokolowski and Fischer [7]) and at liquid–vapor interfaces by DF theory (e.g., Telo da Gama and Evans [8]) or by gradient theory (Cornelisse [9]). Wetting has also been studied experimentally by Schmidt and Moldover [10] for liquid–vapor interfaces and by Taborek and Rutledge [11] for solid-fluid interfaces. Surveys of experimental and theoretical work on wetting phenomena are given by Franck [12] and Davis [13].

The agreement of the BGY results for the system CH_4–CF_4 with experimental and theoretical observations in the literature needs to be discussed. Therefore, liquid–vapor and liquid–liquid interfaces in the vincinity of the three-phase equilibrium, where wetting occurs, are more closely studied in the present paper. The sign of the spreading coefficient, which is calculated from the surface tensions between the various phases of a three-phase equilibrium, determines whether perfect wetting or nonwetting is observed. Therefore, the surface tension is calculated for the different types of interfaces and results are compared to the theories and observations of Cahn and Moldover [14, 15].

In Section 2 the BGY equation and the numerical solution procedure are briefly reviewed. Section 3 gives the molecular model for the system CH_4–CF_4 and introduces the AMFA equation of state. In Section 4 results of liquid–vapor and liquid–liquid interfaces in the system CH_4–CF_4 are discussed. Mainly, the problem of wetting is addressed and results for the surface tension are given.

2. OUTLINE OF METHOD

The BGY equation is used to calculate fluid–fluid interfaces of binary mixtures. Let us consider a mixture of two or more components with the intermolecular potentials $u_{\alpha\beta}(r)$ ($\alpha = a, b, \ldots$, $\beta = a, b, \ldots$). Statistical mechanics gives us expressions for the local densities $n_\alpha(\mathbf{r})$ of the components α, which contain the integration over the Boltzmann factors of all but one particle. Differentiation of n_α with respect to $\mathbf{r}_1$ yields one rigorous BGY equation for each component α [16, 17],

$$\nabla_1 \ln \rho_\alpha(\mathbf{r}_1) = -\sum_\beta \int \rho_\alpha(\mathbf{r}_2)\, g_{\alpha\beta}(\mathbf{r}_1, \mathbf{r}_2)\, \beta \nabla_1 u_{\alpha\beta}(r_{12})\, d\mathbf{r}_2 \tag{1}$$

The approximation scheme of Fischer and Methfessel [2], in an extension to multicomponent mixtures [1, 16], is used. The intermolecular potentials $u_{\alpha\beta}$ are split into their repulsive and attractive parts according to the prescription of Weeks–Chandler–Andersen [18]. The pair correlation functions of the mean attractive forces are set equal to one. The softly repulsive potential is replaced by a hard-sphere potential, and the pair correlation function of the repulsive forces is approximated by the contact value of the pair correlation function $g^{\mathrm{H}}_{\alpha\beta,\,\mathrm{hom}}(r_{12} = d_{\alpha\beta}; \bar{\rho}_a, \bar{\rho}_b, \ldots)$ of a homogeneous hard-sphere fluid at the coarse-grained density $\bar{\rho}_\delta$ ($\delta = a, b, \ldots$). An expression for $g^{\mathrm{H}}_{\alpha\beta,\,\mathrm{hom}}(r_{12} = d_{\alpha\beta}; \bar{\rho}_a, \bar{\rho}_b, \ldots)$ derived by Boublík et al. [19] from Carnahan–Starling–Boublík–Mansoori equation [20, 21] is used. Details of the approximation scheme are given elsewhere [1, 3].

The density profiles of the components of a mixture at a liquid–vapor or liquid–liquid interface are the eigensolutions of the BGY equation at a given temperature T and a given bulk liquid concentration phase x_α. The BGY equation is solved numerically by iteration. Forty grid points per molecular diameter (d_{aa}) are used for the numerical integration of the BGY equation, which is performed over a symmetric interval of 15 molecular diameters to each side of the Gibbs dividing surface. In some cases of liquid–vapor interfaces, an asymmetric interval with 15 molecular diameters on the gas side and up to 75 molecular diameters on the liquid side is used. Thus, the density profiles almost yield at their boundaries the orthobaric bulk densities and concentrations.

The surface tension of a multicomponent system can be calculated from the density profiles by (Ono and Kondo [22])

$$\beta\gamma = \frac{1}{4} \sum_\alpha \sum_\beta \int dz_1 \int d\mathbf{r}_2\, \rho_\alpha(\mathbf{r}_1)\, \rho_\beta(\mathbf{r}_2)\, g_{\alpha\beta}(\mathbf{r}_1, \mathbf{r}_2)\, \beta \frac{du_{\alpha\beta}(r_{12})}{dr_{12}} \frac{r_{12}^2 - 3z_{12}^2}{r_{12}} \tag{2}$$

if the pair correlation functions are approximated in the same way as in the BGY equation.

3. MOLECULAR MODEL AND AMFA EQUATION OF STATE

The intermolecular forces are described by the Lennard–Jones (LJ) potential

$$u_{\alpha\beta}(r) = 4\varepsilon_{\alpha\beta}\left[\left(\frac{\sigma_{\alpha\beta}}{r}\right)^{12} - \left(\frac{\sigma_{\alpha\beta}}{r}\right)^{6}\right] \tag{3}$$

where the unlike interactions are calculated according to the combining rules,

$$\varepsilon_{\alpha\beta} = \xi\sqrt{\varepsilon_{\alpha\alpha}\varepsilon_{\beta\beta}}, \qquad \sigma_{\alpha\beta} = \tfrac{1}{2}\eta(\sigma_{\alpha\alpha} + \sigma_{\beta\beta}) \tag{4}$$

The LJ parameters were used elsewhere [3]:

$$\begin{aligned} \sigma_{\mathrm{CF}_4} &= 4.1910\ \text{Å}, & \varepsilon_{\mathrm{CF}_4}/k &= 203.68\ \mathrm{K} \\ \sigma_{\mathrm{CF}_4}/\sigma_{\mathrm{CH}_4} &= 1.1, & \varepsilon_{\mathrm{CF}_4}/\varepsilon_{\mathrm{CH}_4} &= 1.3586 \\ \eta &= 0.9054, & \xi &= 1.0 \end{aligned} \tag{5}$$

For the numerical solution of the BGY equation, the hard-sphere diameters are set to $d_{\alpha\alpha} = \sigma_{\alpha\alpha}$. No cutoff is used for the LJ potential. Hence, for this molecular model, the bulk phase equilibria can be calculated from the AMFA equation of state:

$$A^{\mathrm{res}} = A^{\mathrm{res}}_{\mathrm{H}} + Npa \tag{6}$$

For the hard-body part, $A^{\mathrm{res}}_{\mathrm{H}}$, the Carnahan–Starling–Boublík–Mansoori equation [20, 21] is used, and for the attractive energy part, Npa, a van der Waals-type expression is derived from the model used in the attractive mean field approximation. The formulation of the AMFA equation of state is given elsewhere [1]. The AMFA equation of state is exact for the model, hard spheres plus attractive mean field approximation, which is used to approximate the BGY equation. Therefore, it can be used to check the accuracy of the numerical solution of the BGY equation and to anticipate the bulk phase behavior of the molecular model. With the AMFA equation of state a liquid–liquid immiscibility was found for CH_4–CF_4, as can be expected from the strong negative deviation from the Lorentz–Berthelot rule ($\eta = 0.9054$). Thus, a necessary condition for wetting is fulfilled.

4. RESULTS AND DISCUSSION

In a previous paper [3] results for liquid–liquid ($\mathrm{L}_1\mathrm{L}_2$) and liquid–vapor ($\mathrm{L}_1\mathrm{V}$) interfaces of the system CH_4(a)–CF_4(b) at 0.02 MPa

($p\sigma_{\mathrm{aa}}^3/\varepsilon_{\mathrm{aa}} = 0.00145$) and 0.10133 MPa ($p\sigma_{\mathrm{aa}}^3/\varepsilon_{\mathrm{aa}} = 0.00734$), calculated with the BGY equation and corresponding bulk phase equilibria with the AMFA equation of state, were presented. The results for the bulk-phase properties with both methods were in good to excellent agreement, as can also be seen from the isobaric temperature versus concentration diagrams in Figs. 1 and 2. At the higher pressure of 0.10133 MPa in Fig. 2, there is simpler phase behavior with a liquid–liquid equilibrium region at lower temperatures which ends in an upper critical solution temperature of about $kT/\varepsilon_{\mathrm{aa}} = 0.791$ and a liquid–vapor region between $kT/\varepsilon_{\mathrm{aa}} = 0.899$ and 1.22. At 0.02 MPa, shown in Fig. 1, there is more complicated phase behavior with a liquid–vapor region, which is now found at lower temperatures, and a liquid–liquid region, which does not vary significantly with pressure. Both regions intersect at $kT/\varepsilon_{\mathrm{aa}} = 0.75826$, which results in a three-phase equilibrium L_1L_2V between two liquids and a vapor and two types of liquid–vapor equilibria, L_1V at temperatures above the three-phase equilibrium and L_2V at lower temperatures.

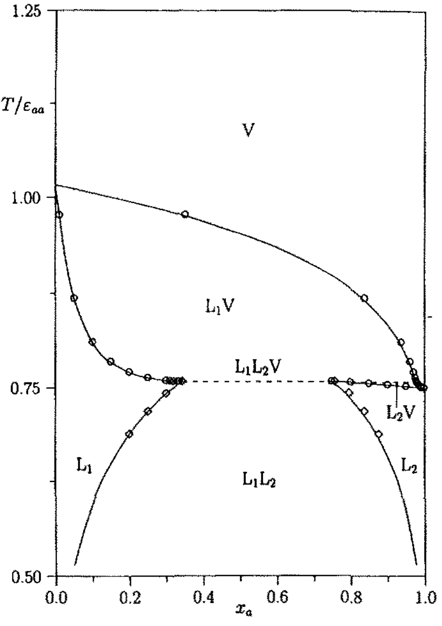

Fig. 1. Temperature vs. concentration diagram for the LJ mixture CH_4(a)–CF_4(b) at $p\sigma_{\mathrm{aa}}^3/\varepsilon_{\mathrm{aa}} = 0.00145$ (0.02 MPa). BGY results [L_1V, L_2V (○); L_1L_2 (◇)] are compared with bulk phase equilibria from AMFA equation of state [L_1V, L_2V, L_1L_2 (—); L_1L_2V (- - -)].

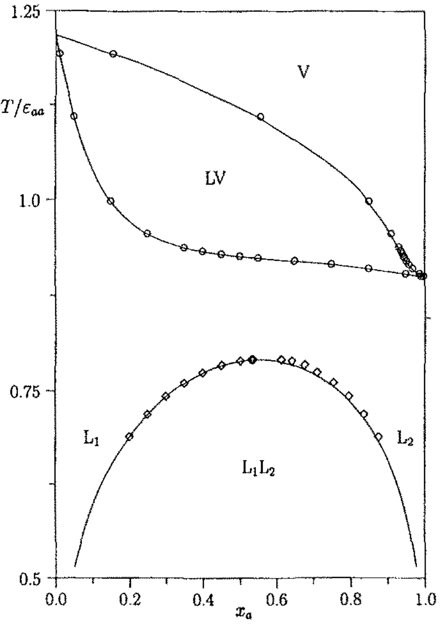

Fig. 2. Temperature vs. concentration diagram for the LJ mixture CH_4(a)–CF_4(b) at $p\sigma_{aa}^3/\varepsilon_{aa} = 0.00734$ (0.10133 MPa). BGY results [LV (○); L_1L_2 (◇)] are compared with bulk phase equilibria from AMFA equation of state [LV, L_1L_2 (—)].

In the present paper results at 0.02 MPa in the vincinity of the three-phase equilibrium are more thoroughly studied. Figure 3 gives density profiles of liquid–vapor interfaces of the type L_1V for bulk liquid concentrations of CH_4(a) from $x_a = 0.01$ to 0.30. Only the profiles of the total density and the partial density of CH_4 are given. Results for the density profile of CF_4 are omitted to avoid confusion. At low CH_4 concentrations the total density decreases with slight oscillations from the bulk liquid to the bulk vapor density, while the partial density profile of CH_4 has—even at very low concentrations of CH_4 (e.g., $x_a = 0.01$)—a maximum in the interface. With increasing x_a, this maximum increases in height and thickness. At about $x_a = 0.20$, a maximum in the total density also appears. The maxima grow until their height corresponds roughly to the density and concentration of the second liquid phase L_2. With values of x_a close to the AMFA results for the three-phase equilibrium ($x_a = 0.343$), these maxima form a broad layer of constant density and concentration as can be seen from Fig. 4. The result at $x_a = 0.336$ (see also Fig. 5) is the closest to the

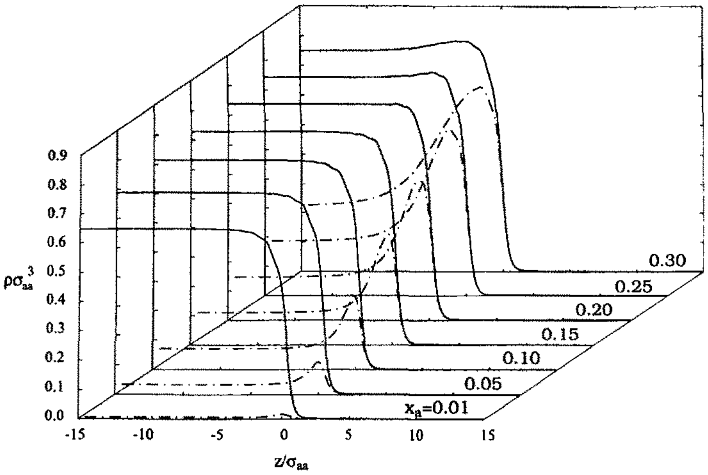

Fig. 3. Total (——) and CH$_4$ partial (- · · -) density profiles of the liquid-vapor interface L$_1$V for the LJ mixture CH$_4$(a)–CF$_4$(b) at $p\sigma_{aa}^3/\varepsilon_{aa} = 0.00145$ (0.02 MPa) and at CH$_4$ concentrations between $x_a = 0.01$ and 0.30 obtained from the BGY equation.

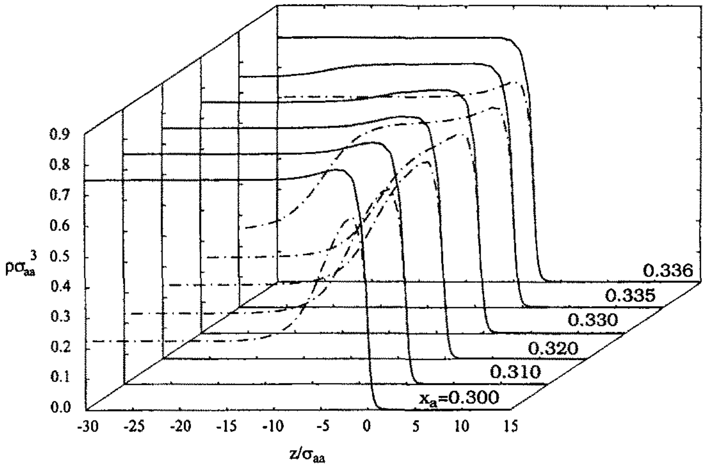

Fig. 4. Total (—) and CH$_4$ partial (· — ·) density profiles of the liquid-vapor interface L$_1$V for the LJ mixture CH$_4$(a)-CF$_4$(b) at $p\sigma_{aa}^3/\varepsilon_{aa} = 0.00145$ (0.02 MPa) and at CH$_4$ concentrations between $x_a = 0.30$ and 0.336 obtained from the BGY equation.

Table I. Comparison of Results for Liquid–Liquid and Liquid–Vapor Interfaces for the LJ Mixture CH_4(a)–CF_4(b) at $p\sigma_{aa}^3/\varepsilon_{aa} = 0.00145$ (0.02 MPa) Near the Three-Phase Equilibrium Obtained from the BGY Equation with Results for the Three-Phase Equilibrium from the AMFA Equation of State (EOS, $kT/\varepsilon_{aa} = 0.75826$)

EOS				BGY				
Type	Phase	x_a	$\rho\sigma_{aa}^3$	Type	Phase	x_a	$\rho\sigma_{aa}^3$	$\gamma\sigma_{aa}^3/\varepsilon_{aa}$
L_1L_2V	L_1	0.34297	0.75400	L_1V	L_1	0.33600	0.75331	
	L_2	0.74780	0.79458		Layer	0.7566	0.7955	1.149
	V	0.97677	0.00194		V	0.97794	0.00196	
L_1L_2V	L_1	0.34297	0.75400	L_1L_2	L_1	0.34297	0.75400	0.020
	L_2	0.74780	0.79458		L_2	0.76521	0.79705	
L_1L_2V	L_2	0.74780	0.79458	L_2V	L_2	0.74780	0.79459	1.132
	V	0.97677	0.00194		V	0.97784	0.00196	

three-phase equilibrium we found with the BGY equation. Here the layer has almost the same density and concentration as the second liquid phase L_2 in the three-phase equilibrium. Results for the bulk phases and the layer with the BGY equation at $x_a = 0.336$ are compared in Table I to the AMFA equation of state results for the three-phase equilibrium, and they agree well. Thus, the layer between the bulk phases L_1 and V is a thin layer of a third wetting phase L_2. For a liquid–vapor interface near a liquid–liquid–vapor equilibrium, wetting can be expected. One of the two liquid

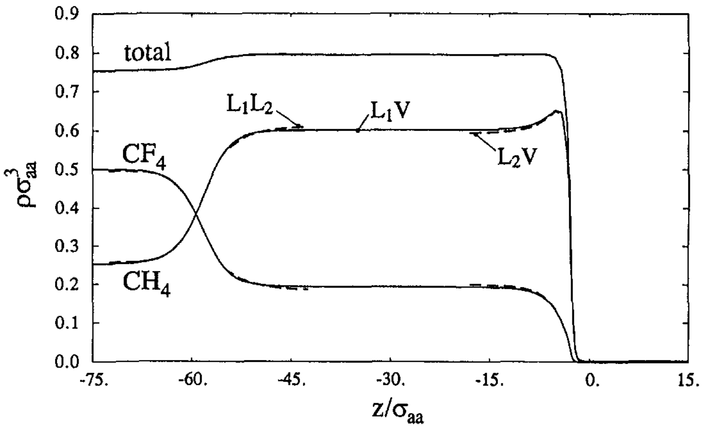

Fig. 5. Density profiles of liquid–liquid and liquid–vapor interfaces for the LJ mixture CH_4(a)–CF_4(b) at $p\sigma_{aa}^3/\varepsilon_{aa} = 0.00145$ (0.02 MPa) near the three-phase equilibrium obtained from the BGY equation.

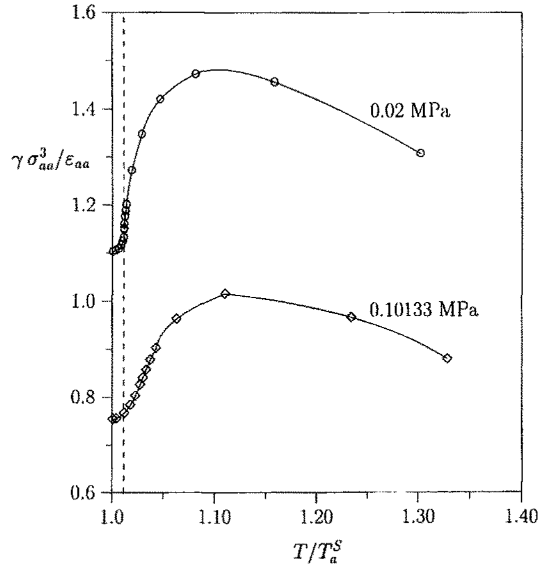

Fig. 6. Surface tension vs. temperature diagram for the LJ mixture CH_4(a)–CF_4(b) at $p\sigma_{aa}^3/\varepsilon_{aa} = 0.00145$ [0.02 MPa (○)] and $p\sigma_{aa}^3/\varepsilon_{aa} = 0.00734$ [0.10133 MPa (◇)] obtained from the BGY equation. The location of the three-phase equilibrium is marked for convenience (- - -).

phases, here L_2, is perfectly wetting the other liquid phase, L_1. In Fig. 5 BGY results for the other two types of interfaces—L_1L_2 and L_2V—which make up the three-phase equilibrium are also shown. The density profiles for L_1L_2 and L_2V agree well with the result for L_1V, which is also confirmed by the bulk phase results in Table I.

The surface tensions of the liquid–vapor interfaces for both isobars are compared in Fig. 6. Results for both isobars are similar, but while the curve is continuous for 0.10133 MPa, there is a discontinuity at the temperature of the three-phase equilibrium for 0.02 MPa. The surface tension γ_{L_1V} of the L_1V interface decreases and the surface tension γ_{L_2V} of the L_2V interface increases while the three-phase equilibrium is approached. Finally, when wetting occurs, the difference at the discontinuity is $\gamma_{L_1V} - \gamma_{L_2V} = 0.017$ (see Table I), which is equal to $\gamma_{L_1L_2} = 0.020$ within the uncertainty of the calculations. This result is in agreement with the theory of Cahn [14].

In the case of equilibrium between two liquids—L_1 and L_2—and a vapor V, the following relationship must be fulfilled:

$$\gamma_{L_1V} \leqslant \gamma_{L_1L_2} + \gamma_{L_2V} \tag{7}$$

Phase L_2 is not wetting the interface L_1V, as long as the inequality in Eq. (7) holds. In the case of equality (Antonov's rule), phase L_2 will wet the L_1V interface. Equation (7) can also be written as

$$\gamma_{L_1V} - \gamma_{L_2V} \leqslant \gamma_{L_1L_2} \tag{8}$$

Cahn [14] argues that, if the critical point $L_1 = L_2$ is aproached, both, $\gamma_{L_1L_2}$ and $\gamma_{L_1V} - \gamma_{L_2V}$, will vanish as

$$\begin{aligned} \gamma_{L_1L_2} &\propto (T_C - T)^{\mu} \\ \gamma_{L_1V} - \gamma_{L_2V} &\propto (T_C - T)^{\beta} \end{aligned} \tag{9}$$

where μ is about 1.3 and β is in the range 0.3 to 0.4. As $\gamma_{L_1L_2}$ decreases more rapidly than $\gamma_{L_1V} - \gamma_{L_2V}$, the inequality will become an equality at a temperature below the $L_1 = L_2$ critical temperature. Thus, perfect wetting of L_2 in the L_1V interface does occur. This theory was later experimentally verified by Moldover and Cahn [15] for the system methanol–cyclohexane. The present results are in agreement with the theory of Cahn. Phase L_2 is wetting the L_1V interface at a temperature of $kT/\varepsilon_{aa} = 0.7583$, which is not far below the critical temperature $kT_C/\varepsilon_{aa} = 0.791$. The results with the BGY equation for the surface tension between the different phases fulfill Antonov's rule [the equality in the relationship, Eq. (7)], as shown above.

A still open question is, Why is L_2 wetting L_1V instead of L_1 wetting L_2V? This can be unterstood from the surface tensions: far away from the conditions of three-phase equilibrium, the interface L_1V has, with $\gamma\sigma_{aa}^3/\varepsilon_{aa} \approx 1.4$, a higher surface tension than the interface L_2V, with $\gamma\sigma_{aa}^3/\varepsilon_{aa} \approx 1.1$ (see Fig. 6), while the interface L_1L_2 has only a very low surface tension with $\gamma\sigma_{aa}^3/\varepsilon_{aa} \approx 0.02$. When the conditions are changed toward the three-phase equilibrium, γ_{L_1V} is decreasing while γ_{L_2V} is only slightly increasing, until Antonov's rule is fulfilled in the three-phase equilibrium and perfect wetting occurs. The decrease in γ_{L_1V} is achieved by the occurrence of the maxima in the interface L_1V which grow to a wetting layer of L_2. Thus, in three-phase equilibrium the interface L_1V consists, in fact, of two interfaces, L_1L_2 and L_2V (compare Fig. 5), and the surface tension γ_{L_1V} is the sum of the other two (Antonov's rule). The same would happen if a wetting layer of L_1 would occur in L_2V. Then the surface tension of L_2V would increase until Antonov's rule is fulfilled. But, in the second case, the energy of the system would increase, while decreasing in the first case. Thus, the wetting of the surface with the higher surface tension (here, L_1V) is energetically more favorable.

Wetting of a liquid–vapor interface has also been studied theoretically by Telo da Gama and Evans [8] and by Tarazona et al. [23, 24] with local DF theories and by Cornelisse [9] with a gradient theory. Telo da Gama and Evans parametrized the total and the partial density profiles of the less volatile species with monotonic tanh functions in order to simplify the calculations. Thus, monotonic behavior is anticipated and a fully developed wetting layer is suppressed. Tarazona et al. used the DF theory of Sullivan [25], which is somewhat simpler than the one of Telo da Gama and Evans and was used without parametrization. Also, it is linked to a consistent van der Waals-type equation of state which is similar to the AMFA equation of state. With this theory, wetting with a second liquid phase of a smaller molar density was found. Cornelisse used a gradient theory in combination with the Peng–Robinson or the APACT equation of state. He found wetting with a denser liquid phase L_2 in the interface L_1V, very similar to the present results, for the systems CO_2–decane, water–hexane, water–benzene, and water–ethanol–hexane. Using a mixing parameter β_{ij} equal to 0.0 for the influence parameter c_{ij} in the gradient theory, Cornelisse always found wetting under three-phase equilibrium conditions with both equations of state. Using a different β_{ij} sometimes yielded wetting, but more often no wetting layer was found. A still open question is whether the BGY equation in the Fischer–Methfessel approximation will always yield wetting in systems with three-phase equilibrium. With the BGY equation, wetting at solid–gas interfaces was also found for pure argon at carbon and at CO_2 walls [5] and for binary model mixtures at carbon walls [26]. Thus, we expect to find wetting with the BGY equation in the Fischer–Methfessel approximation also for other fluid systems which show liquid–liquid immiscibility, i.e., three-phase equilibrium. Liquid–liquid immiscibility depends, as mentioned in Section 3, on the intermolecular forces and can be expected with strong deviations from the Lorentz–Berthelot rule.

5. CONCLUSION

The BGY equation in combination with the consistent AMFA equation of state has again been proven to be an interesting tool to investigate interfaces and wetting phenomena. In the system CH_4–CF_4 the formation of a perfectly wetting layer has been studied and is shown in three-dimensional plots. Furthermore, the surface tension has been calculated. The results are in agreement with the phenomenological theory of wetting by Cahn [14] and other theoretical investigations.

ACKNOWLEDGMENT

The author would like to thank Professor J. Fischer for helpful discussion.

REFERENCES

1. M. Wendland, *Fluid Phase Equil.* **141**:25 (1997).
2. J. Fischer and M. Methfessel, *Phys. Rev. A* **22**:2836 (1980).
3. M. Wendland, *Fluid Phase Equil.* **147**:105 (1998).
4. G. F. Teletzke, L.-E. Scriven, and H. T. Davis, *J. Colloid Interface Sci.* **87**:550 (1982).
5. M. Wendland, S. Salzmann, U. Heinbuch, and J. Fischer, *Mol. Phys.* **67**:161 (1989).
6. S. Dhawan, M. E. Reimel, L.-E. Scriven, and H. T. Davis, *J. Chem. Phys.* **94**:4479 (1991).
7. S. Sokolowski and J. Fischer, *Phys. Rev. A* **41**:6866 (1990).
8. M. M. Telo da Gama and R. Evans, *Mol. Phys.* **48**:251 (1983).
9. P. M. W. Cornelisse, Ph.D. thesis (Technische Universiteit Delft, Delft, 1997), pp. 145–203.
10. J. W. Schmidt and M. R. Moldover, *J. Chem. Phys.* **79**:379 (1983).
11. P. Taborek and J. E. Rutledge, *Phys. Rev. Lett.* **68**:2184 (1992).
12. C. Franck, in *Fundamentals of Inhomogeneous Fluids*, D. Henderson, ed. (Marcel Dekker, New York, 1992), pp. 277–302.
13. H. T. Davis, *Statistical Mechanics of Phases, Interfaces, and Thin Films* (VCH, New York, 1996), pp. 599–626.
14. J. M. Cahn, *J. Chem. Phys.* **66**:3667 (1977).
15. M. R. Moldover and J. M. Cahn, *Science* **207**:1073 (1980).
16. S. Sokolowski and J. Fischer, *Mol. Phys.* **70**:1097 (1990).
17. L. Blum and D. Henderson, in *Fundamentals of Inhomogeneous Fluids*, D. Henderson, ed. (Marcel Dekker, New York, 1992), pp. 239–276.
18. J. D. Weeks, D. Chandler, and H. C. Andersen, *J. Chem. Phys.* **54**:5237 (1971).
19. T. Boublík, I. Nezbeda, and K. Hlavaty, *Statistical Thermodynamics of Simple Liquids and Their Mixtures* (Elsevier, Amsterdam, 1980), p. 109.
20. T. Boublík, *J. Chem. Phys.* **53**:471 (1970).
21. G. A. Mansoori, N. F. Carnahan, K. E. Starling, and T. W. Leland, *J. Chem. Phys.* **54**:1523 (1971).
22. S. Ono and S. Kondo, in *Encyclopedia of Physics, Vol. 10*, S. Flügge, ed. (Springer, Berlin, 1960), p. 134.
23. P. Tarazona, M. M. Telo da Gama, and R. Evans, *Mol. Phys.* **49**:301 (1983).
24. P. Tarazona, R. Evans, and U. Marini Bettolo Marconi, *Mol. Phys.* **54**:1357 (1985).
25. D. E. Sullivan, *J. Chem. Phys.* **77**:2632 (1982).
26. M. Wendland, U. Heinbuch, and J. Fischer, *Fluid Phase Equil.* **48**:259 (1989).